Nanoscale Advances

Accepted Manuscript

This article can be cited before page numbers have been issued, to do this please use: Z. Zhang, J. Yu, J. Zhang, Y. Lian, Z. Shi, Z. Cheng and M. Gu, *Nanoscale Adv.*, 2019, DOI: 10.1039/C9NA00635D.

ROYAL SOCIETY OF CHEMISTRY

rsc.li/nanoscale-advances

View Article Online
DOI: 10.1039/C9NA00635D

ARTICLE

PH–controlled growth of triangular silver nanoprism at a large scale

Zhishan Zhang, Ji Yu, Jianhui Zhang*, Yadong Lian, Zeyu Shi, Zimo Cheng, Min Gu*

A simple, mild, and reproducible one–pot approach was developed to synthesize triangular silver nanoprisms (TSNPR) at a large scale. The TSNPR size was tailored from 30 to 100 nm by varying the dosage of sodium hydroxide pentanol solution in the water/polyvinylpyrrolidone/n–pentanol ternary system. The use of sodium hydroxide pentanol solution modified the initial pH of the water/polyvinylpyrrolidone/n–pentanol system, and made the synthesis of TSNPR highly reproducible and independent of the polyvinylpyrrolidone pH. N,N–dimethyl formamide and formamide were used to control the system pH and improved the resultant TSNPRs in both syntheses repeatably and with well defined shape. The extinction bands of the TSNPRs were relatively narrow, which makes them promising for chemical and biological applications.

Introduction

Over recent decades, the shape–controlled synthesis of metallic nanoparticles has shown technological importance because of the strong correlation between size, shape, optical, electrical, chemical, and biological properties[1–4]. Among the metal nanoparticles, silver (Ag) nanoparticles are of particular interest. Because of their unique optical properties such as strong surface plasmon resonance and tunable light absorption by size, triangular silver nanoparticles (TSNPRs) have been used extensively in surface–enhanced Raman scattering, solar cells, conductive fillers in conductive adhesives and thermal interfacial materials, a class of broad–spectrum antimicrobial reagents, classic catalysts, and biological detection[5–14], etc. TSNPRs were first synthesized by Jin and coworkers using a plasmon–mediated method in 2001[15], and different strategies were used to prepare TSNPRs, including optical–induction methods[5,16,17], thermal transformation[18–20], seed–mediated methods[21–24], and template-directed growth[25–27]. However, only a few of these methods can tune the Ag nanoprisms size. The optical–induction methods can produce uniform TSNPRs, but their yields are poor. Furthermore, too many reagents are used in seed–mediated methods. Finally, complex synthesis procedures also limit these methods.

To simplify the synthesis route and to increase the TSNPR yield, we have developed a unique water/polyvinylpyrrolidone (PVP)/n–pentanol ternary system (WWPN) to prepare Ag nanoprisms[28]. The WWPN system has provided simplified synthesis procedures and a significantly increased yield of about 20 mg. The resulting TSNPR is pure and its size can be tuned by adjusting the PVP amount. However, the pH of commercial PVP varies frequently, which is critical for our WWPN system. The pH of different batches of PVP (K30) varies from 3 to 5. When the pH of PVP was less than 3.6, the repeat synthesis of TSNPR in the WWPN system usually fails. The initial pH of the WWPN system must be controlled to ensure the synthesis repeatability. By using the sodium hydroxide–pentanol solution (SHPS) innovatively, we controlled the initial pH of the WWPN system. The TSNPRs can be synthesized repeatedly independent of the PVP pH, and they can be tuned from 30 to 100 nm by adjusting the amount of SHPS. To avoid the following precipitation reaction (1) between $AgNO_3$ and NaOH:

$$2NaOH+2AgNO_3=2NaNO_3+Ag_2O\downarrow+H_2O \quad (1)$$

Before adding $AgNO_3$, the SHPS was added to the n–pentanol solution of PVP to increase the solution pH from 4 to 7. However, as indicated previously[28], most of the resultant TSNPRs were truncated. To improve the synthesis repeatability and triangular shape of the TSNPRs, N,N–dimethyl formamide (DMF) and formamide were used to control the system pH. DMF and formamide helped to synthesize TNPRs repeatedly. The resultant TNPRs showed a well–defined triangular shape. By controlling the initial pH of the WWPN system, the simple, mild, and reproducible one–pot approach was developed to synthesize TNPRs with a tunable size and excellent triangular shape at a large scale.

Experimental

Materials

National Laboratory of Solid State Microstructures and Department of Physics, Collaborative Innovation Center of Advanced Microstructures, Nanjing University, Nanjing 210093, P.R. China ***E–mail address:*** *mgu@nju.edu.cn, zhangjh@nju.edu.cn*

View Article Online
DOI: 10.1039/C9NA00635D

Silver nitrate ($AgNO_3$, AR, ⩾ 99.8%), formamide (⩾ 99.5%), DMF (⩾ 99.5%), ethanol and sodium hydroxide (NaOH, AR, ⩾ 96%) were from Sinopharm Chemical Reagent Co. Ltd. N – pentanol (⩾ 99%) was from Shanghai Lingfeng Chemical Reagent Co. Ltd. Polyvinylpyrrolidone (PVP, Mn=30000 g·mol^{-1}, pH=3.64) was from Shanghai Yeasen Biotechnology Co. Ltd. Water was distilled and deionized using a Millipore Milli–Q Purification System, which has a resistivity of more than 18.2 MΩ·cm. All reagents were used without further purification.

Instruments

Extinction spectra of silver-nanoparticle dispersions were recorded using a UV–1800 spectrophotometer (Mapada). Scanning electron microscopy (SEM, FEI Helios 600i, operating voltage: 2 kV, operating current: 34 pA) was used to observe the morphology of the silver nanoparticles. X-ray diffraction (XRD) was performed in a Philips X'pert Pro using Cu-$K_{\alpha 1}$ radiation (λ=1.5406 Å) from 30 to 90°. Transmission electron microscopy (TEM) images were taken using a JEM–2100 with an acceleration voltage of 200 kV. Samples for TEM analysis were prepared by dripping a drop of silver nanoparticle dispersions onto the copper grids and drying in air at room temperature.

Synthesis of Ag nanoprisms by adding SHPS

In a typical synthesis, 1.8 g of PVP was dissolved in 60 mL of n–pentanol in a conical flask sealed with a ground stopper. A certain amount of SHPS (1 g/L) was injected into the solution with stirring. After 30 min, 3.9 mL of aqueous $AgNO_3$ (1.2 wt%) was added and stirred for 30 min to form the WWPN ternary system. The reaction solution in the sealed flask was placed into a constant–temperature oven and heated at 95°C for about 42 h. The reaction products were washed with ethanol three times by centrifugation, and Ag nanoprisms were obtained.

Synthesis of Ag nanoprisms by adding organic base

0.6 g of PVP was dissolved in 60 mL of n–pentanol in a conical flask sealed with a ground stopper. 3.9 mL of aqueous $AgNO_3$ (0.6 wt%) was added to the solution and stirred for 30 min. The reaction solution in the sealed flask was placed into a constant–temperature oven and heated at 95°C for 12 h. 3 mL of DMF or formamide was added after the reaction solution was cooled to room temperature, and stirred for 5 min. The reaction solution in the sealed flask was placed into a constant – temperature oven and heated at 95°C for a further 50 h (for DMF) or 30 h (for formamide). The final products were washed with ethanol three times by centrifugation, and Ag nanoprisms were obtained.

Results and discussion

Synthesis of Ag nanoprisms by changing pH

Fig. 1 shows typical TEM and SEM images of Ag nanoprisms made with different amounts of SHPS. As shown in Fig. 1a–f, Ag nanoprisms with average edge lengths of 30 ± 4 nm, 35 ± 5 nm, 45 ± 6 nm, 50 ± 7 nm, 60 ± 8 nm, 70 ± 9 nm, 80 ± 12 nm and 100 ± 20 nm were synthesized by using 0.25 mL, 0.375 mL, 0.5 mL, 0.75 mL, 1 mL, 1.25 mL, 1.5 mL and 2 mL of SHPS, respectively. However, when SHPS was not added into the WWPN system, the synthesis of TSNPR failed, when the amount of SHPS was equal to or greater than 2.5 mL, a black precipitate was formed, indicating that silver oxide was precipitated. The influence of SHPS amount on the nanoprism edge lengths are illustrated by linearly fitting with the following formula:

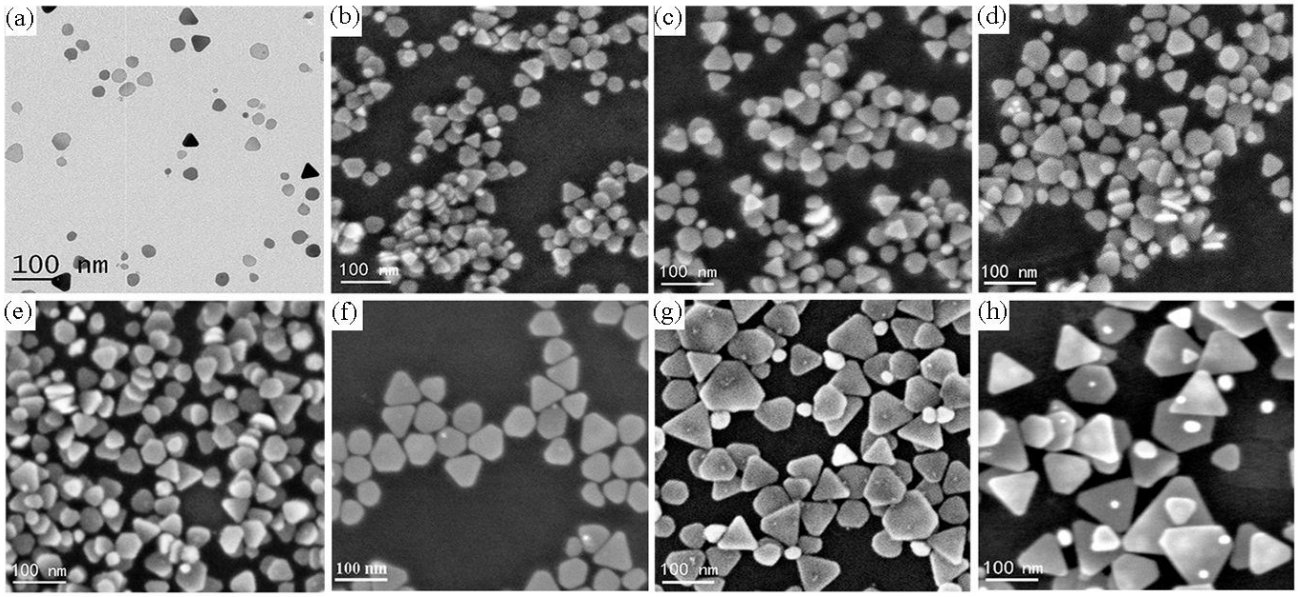

Fig. 1 TEM and SEM images of Ag nanoprisms made with (a) 0.25 mL, (b) 0.375 mL, (c) 0.5 mL, (d) 0.75 mL, (e) 1.0 mL, (f) 1.25 mL, (g) 1.5 mL and (h) 2.0mL of SHPS. The average edge length of the corresponding Ag nanoprisms is (a) 30 ± 4 nm, (b) 35 ± 5 nm, (c) 45 ± 6 nm, (d) 50 ± 7 nm, (e) 60 ±8 nm, (f) 70 ± 9 nm, (g) 80 ± 12 nm and (h) 100 ± 20 nm.

$$y=21.47+39.12x \quad (2)$$

View Article Online
DOI: 10.1039/C9NA00635D

where y (nm) refers to the nanoprism edge length, and x (mL) refers to the SHPS amount. The correlation coefficient is 0.997.

Photographs of ethanol dispersions of Ag nanoprisms with different average edge lengths are shown in Fig. 2a. These dispersions vary in color with their LSPR properties, from pink and purple, to blue. The in–plane dipole plasmon resonance band of the Ag nanoprisms red-shifts with the increase of the average edge length of the Ag nanoprisms. Fig. 2b shows the extinction spectra for ethanol dispersions of Ag nanoprisms with different average edge lengths. Every spectral line has three distinctive peaks, a large strong peak at a long wavelength, a weaker broad peak, and a small sharp peak at a short wavelength. These peaks can be assigned to the in–plane dipolar, in–plane quadrupolar, and out–of–plane quadrupolar plasmon resonance bands, respectively[28]. As shown in Fig. 2b, the in–plane dipole plasmon–resonance peak blue-shifts to a short wavelength with an increase in amount of SHPS. The prominent (111) reflection of Ag nanoprisms at 2θ = 38.2° in Fig. 2c, shows that (111) plane is the preferred orientation surface.

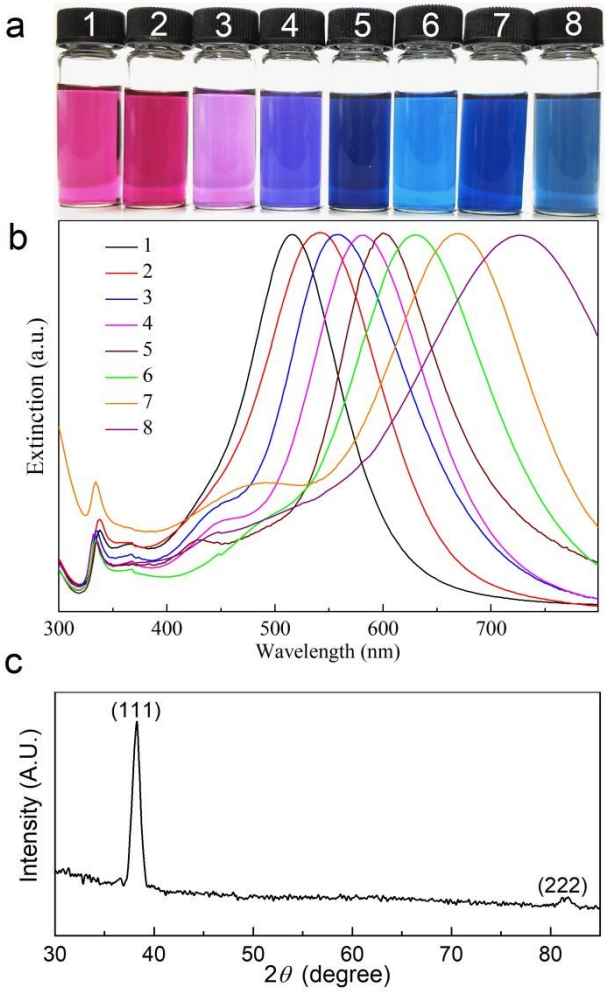

Fig. 2(a) Photographs and (b) extinction spectra for ethanol dispersions of Ag nanoprisms with average edge length of (1) 30 ± 4 nm, (2) 35 ± 5 nm, (3) 45 ± 6 nm, (4) 50 ± 7 nm, (5) 60 ±8 nm, (6) 70 ± 9 nm, (7) 80 ± 12 nm and (8) 100 ± 20 nm, respectively. (c) XRD patterns of the Ag nanoprisms

As shown in Fig. 1b–f, most Ag nanoprisms made with SHPS were truncated. To obtain regular triangular Ag nanoprisms with sharp corners, DMF and formamide were investigated to improve the triangular shape of the Ag nanoprisms. DMF had been demonstrated as a solvent and reducing agent in the presence of PVP, and has changed the preferential adsorption of PVP to {111} Ag facets[29]. Pastoriza–Santos and coworkers proposed the mechanism outlined in formula (3)[20]:

$$HCONMe_2(DMF)+2Ag^+ + H2O \rightarrow 2A^0 + Me_2NCOOH + 2H^+ \quad (3)$$

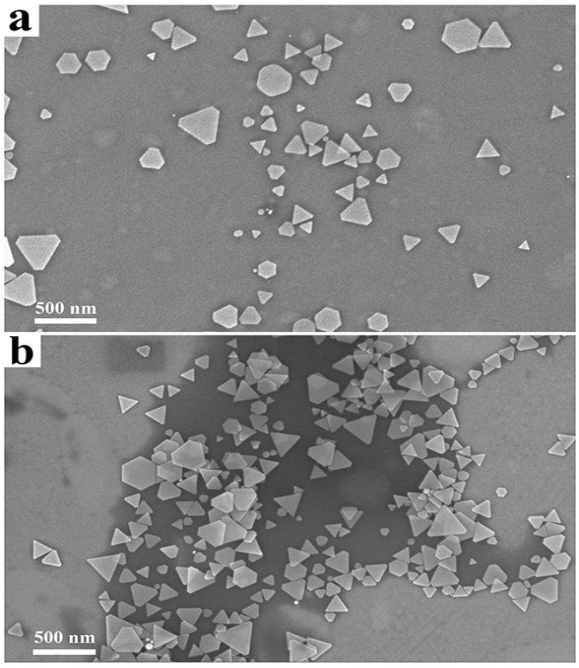

Fig. 3 SEM images of Ag nanoprisms made with 0.6 g PVP and different annexing agent. (a) 3 mL DMF, (b) 3 mL formamide.

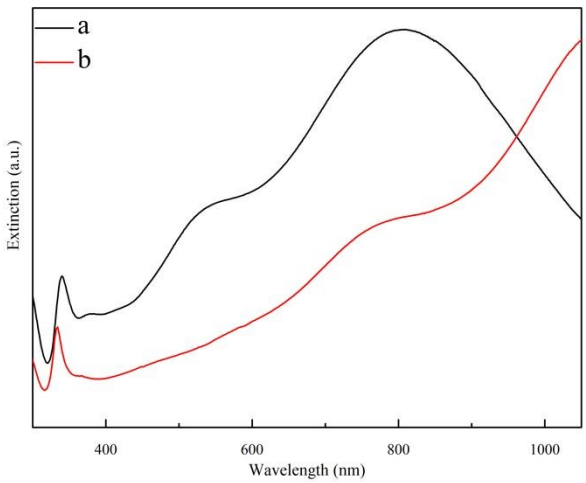

Fig. 4 Extinction spectra for ethanol solutions of Ag nanoprisms made with 0.6 g PVP and different annexing agent. (a) 3 mL DMF, (b) 3 mL formamide.

As shown in Fig. 3a and Fig. 4a, the SEM and extinction spectra show that the Ag nanoprisms made with DMF had a well–defined shape with sharp corners but an uneven

View Article Online
DOI: 10.1039/C9NA00675D

size. As shown in Fig. 3b and Fig. 4b, the use of formamide improved the triangular shape of the Ag nanoprisms, but expanded the size-distribution range and led to broad extinction bands.

Mechanism of the synthesis of Ag nanoprisms by changing the pH

Typically, the growth mechanisms of Ag nanoprisms can be divided into crystallographic and redox–chemistry arguments. Each methodology involves two general steps. One is nucleation of nanoprism seeds, and the other is crystal growth of seeds by a mediated reduction of metal ions[30,31]. In the first step of the synthesis, when the reaction solution was heated, Ag^+ ions diffused into the WWPN ternary system region and reacted with PVP by coordinating with O and N atoms of the pyrrolidone ring of PVP, and the Ag^+–PVP complex was formed[32]. Ag^+–PVP was reduced to Ag^0–PVP. The reactions may follow formulae (4) and (5)[33,34].

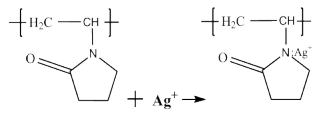

(4)

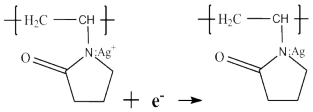

(5)

H^+ ions formed ceaselessly as the reaction proceeded. An increased amount of H^+ ions in the system depresses the reduction reaction, and ultimately, Ag nanoprisms growth. Therefore, the pH of the reaction system can affect the reduction rate. When the pH of the reaction solution increased, the concentration of H^+ ions in the reaction system decreased, the reaction proceeded in the reduction direction, which promoted the growth of Ag nanoprism. Therefore, as the amount of SHPS increases, the size of the triangular Ag nanoprism becomes larger. When the nucleation of nanoprism seeds and the crystal growth of seeds by the mediated reduction of metal ions reached a balance, Ag nanoprisms with a certain size were obtained. On the other hand, it is evident that the corners of the Ag nanoprisms were poorly truncated. It can be ascribed to the acidic environment caused by the H^+ ions formation. With the pH values decreasing, namely the amount of H^+ increasing, equal to the etchant ability being stronger, and the truncation reaction is more likely to occur. The truncated nanoprism would further transform into a nanodisc[35]. Thus, as seen from the SEM images, when the amount of SHPS was equal to or less than 0.25 mL, truncated nanoprisms with round tips formed, and even some Ag nanospheres, rather than nanoprisms.

All the above experimental approaches were targeted towards controlling the initial pH of the reaction solution. The results proved that the higher initial pH led to the formation of Ag nanoprisms. Therefore, the pH controls the triangular Ag nanoprisms growth.

The discussion above indicates that the Ag nanoprisms made by adding SHPS were size–tunable with a narrow size distribution but were truncated. The Ag nanoprisms made by adding organic base had a well–defined shape with sharp corners but had a polydisperse size distribution. It is expected that the high-purity, uniform Ag nanoprisms with sharp corners can be obtained by combining the advantages of both methods mentioned above and reducing the shortcomings.

Conclusions

By controlling the initial pH, the WWPN ternary system was developed to prepare TSNPRs reproducibly with a tunable size and a well-defined triangular shape at a large scale. SHPS, DMF, and formamide were used to control the initial pH. Ag nanoprisms made with SHPS were monodisperse, and tunable in size, but their corners were usually truncated. The Ag nanoprisms made with DMF or formamide had a well-defined triangular shape, but they tended to be polydisperse.

Acknowledgements

This project was supported by the National Basic Research Program of China through Grant no. 2016YFA0201604.

References

1 Y. Sun, *Science (80-.).*, 2002, **298**, 2176–2179
2 K. L. Kelly, E. Coronado, L. L. Zhao and G. C. Schatz, *J. Phys. Chem. B*, 2003, **107**, 668–677.
3 M. Rycenga, C. M. Cobley, J. Zeng, W. Li, C. H. Moran, Q. Zhang, D. Qin and Y. Xia, *Chem. Rev.*, 2011, **111**, 3669–3712.
4 W. L. Barnes, A. Dereux and T. W. Ebbesen, *Nature.*,2003, **424**, 824–830.
5 A. P. Kulkarni, K. M. Noone, K. Munechika, S. R. Guyer and D. S. Ginger, *Nano Lett.*, 2010, **10**, 1501–1505.
6 K. Yao, M. Salvador, C.-C. Chueh, X.-K. Xin, Y.-X. Xu, D. W. DeQuilettes, T. Hu, Y. Chen, D. S. Ginger and A. K. Y. Jen, *Adv. Energy Mater.*, 2014, **4**, 1400206.
7 S. C. Boca, M. Potara, A.-M. Gabudean, A. Juhem, P. L. Baldeck and S. Astilean, *Cancer Lett.*, 2011, **311**, 131–140.
8 C. Gao, Z. Lu, Y. Liu, Q. Zhang, M. Chi, Q. Cheng and Y. Yin, *Angew. Chemie - Int. Ed.*, 2012, **51**, 5629–5633
9 C. Zhang, J. Zhu, J. Li and J. Zhao, *ACS Appl. Mater. Interfaces*, 2017, **9**, 17387–17398.
10 M. Stavytska-Barba, M. Salvador, A. Kulkarni, D. S. Ginger and A. M. Kelley, *J. Phys. Chem. C*, 2011, **115**, 20788–20794.
11 P. Christopher, H. Xin and S. Linic, *Nat. Chem.*, 2011, **3**, 467–472
12 L. Liu, J. Yang, J. Xie, Z. Luo, J. Jiang, Y. Y. Yang and S. Liu, *Nanoscale*, 2013, **5**, 3834.

View Article Online
DOI: 10.1039/C9NA00635D

13 M. Potara, S. Boca, E. Licarete, A. Damert, M. C. Alupei, M. T. Chiriac, O. Popescu, U. Schmidt and S. Astilean, *Nanoscale*, 2013, **5**, 6013–6022.
14 S. Liu, R. Jiang, P. You, X. Zhu, J. Wang and F. Yan, *Energy Environ. Sci.*, 2016, **9**, 898–905.
15 R. Jin, *Science (80-.).*, 2001, **294**, 1901–1903.
16 C. Xue and C. A. Mirkin, *Angew. Chemie Int. Ed.*, 2007, **46**, 2036–2038.
17 R. Jin, Y. Charles Cao, E. Hao, G. S. Métraux, G. C. Schatz and C. A. Mirkin, *Nature*, 2003, **425**, 487–490.
18 Y. Sun, B. Mayers and Y. Xia, *Nano Lett.*, 2003, **3**, 675–679.
19 G. S. Mtraux and C. a Mirkin, *Adv. Mater.*, 2005, **17**, 412–415.
20 A. Sarkar, S. Kapoor and T. Mukherjee, *J. Colloid Interface Sci.*, 2005, **287**, 496–500.
21 X. Liu, L. Li, Y. Yang, Y. Yin and C. Gao, *Nanoscale*, 2014, **6**, 4513–4516.
22 Q. Zhang, Y. Hu, S. Guo, J. Goebl and Y. Yin, *Nano Lett.*, 2010, **10**, 5037–5042.
23 J. Zeng, X. Xia, M. Rycenga, P. Henneghan, Q. Li and Y. Xia, *Angew. Chemie - Int. Ed.*, 2011, **50**, 244–249.
24 C. Gao, J. Goebl and Y. Yin, *J. Mater. Chem. C*, 2013, **1**, 3898–3909.
25 T. C. Deivaraj, N. L. Lala and J. Y. Lee, *J. Colloid Interface Sci.*, 2005, **289**, 402–409.
26 S. Chen and D. L. Carroll, *Nano Lett.*, 2002, **2**, 1003–1007.
27 X. Jiang, Q. Zeng and A. Yu, *Nanotechnology*, 2006, **17**, 4929–4935.
28 J. Zhang, H. Liu, P. Zhan, Z. Wang and N. Ming, *Adv. Funct. Mater.*, 2007, **17**, 1558–1566.
29 M. Tsuji, X. Tang, M. Matsunaga, Y. Maeda and M. Watanabe, *Cryst. Growth Des.*, 2010, **10**, 5238–5243.
30 J. E. Millstone, S. J. Hurst, G. S. Métraux, J. I. Cutler and C. A. Mirkin, *Small*, 2009, **5**, 646–664.
31 Y. Sun, *Chem. Soc. Rev.*, 2013, **42**, 2497–2511.
32 B. Yin, H. Ma, S. Wang and S. Chen, *J. Phys. Chem. B*, 2003, **107**, 8898–8904.
33 Y. Sun and Y. Xia, *Adv. Mater.*, 2003, **15**, 695–699.
34 H. Wang, X. Qiao, J. Chen, X. Wang and S. Ding, *Mater. Chem. Phys.*, 2005, **94**, 449–453.
35 Y. Chen, C. Wang, Z. Ma and Z. Su, *Nanotechnology*, 2007, **18**, 325602.